PROCEEDINGS B

rspb.royalsocietypublishing.org

Research

Cite this article: Rode C, Siebert T, Tomalka A, Blickhan R. 2016 Myosin filament sliding through the Z-disc relates striated muscle fibre structure to function. *Proc. R. Soc. B* **283**: 20153030.
http://dx.doi.org/10.1098/rspb.2015.3030

Received: 18 December 2015
Accepted: 5 February 2016

Subject Areas:
theoretical biology, biomechanics, structural biology

Keywords:
striated muscle fibre, sliding filament theory, Z-disc, model, myofilaments

Author for correspondence:
Christian Rode
e-mail: christian.rode@uni-jena.de

Electronic supplementary material is available at http://dx.doi.org/10.1098/rspb.2015.3030 or via http://rspb.royalsocietypublishing.org.

THE ROYAL SOCIETY PUBLISHING

Myosin filament sliding through the Z-disc relates striated muscle fibre structure to function

Christian Rode[1], Tobias Siebert[2], Andre Tomalka[2] and Reinhard Blickhan[1]

[1]Department of Motion Science, Friedrich-Schiller-University Jena, Jena 07749, Thuringia, Germany
[2]Institute of Sport- and Movement Science, University of Stuttgart, Stuttgart 70174, Baden-Wuerttemberg, Germany

Striated muscle contraction requires intricate interactions of microstructures. The classic textbook assumption that myosin filaments are compressed at the meshed Z-disc during striated muscle fibre contraction conflicts with experimental evidence. For example, myosin filaments are too stiff to be compressed sufficiently by the muscular force, and, unlike compressed springs, the muscle fibres do not restore their resting length after contractions to short lengths. Further, the dependence of a fibre's maximum contraction velocity on sarcomere length is unexplained to date. In this paper, we present a structurally consistent model of sarcomere contraction that reconciles these findings with the well-accepted sliding filament and crossbridge theories. The few required model parameters are taken from the literature or obtained from reasoning based on structural arguments. In our model, the transition from hexagonal to tetragonal actin filament arrangement near the Z-disc together with a thoughtful titin arrangement enables myosin filament sliding through the Z-disc. This sliding leads to swivelled crossbridges in the adjacent half-sarcomere that dampen contraction. With no fitting of parameters required, the model predicts straightforwardly the fibre's entire force–length behaviour and the dependence of the maximum contraction velocity on sarcomere length. Our model enables a structurally and functionally consistent view of the contractile machinery of the striated fibre with possible implications for muscle diseases and evolution.

1. Background

As motors of life, muscles convert chemical energy into mechanical energy and heat. Muscles transport substances within the body, stabilize the skeleton and enable locomotion. The first property characterizing the mechanical function of striated muscles to be described [1] was the active isometric force–length relationship (FLR). This property shows the maximal forces the striated muscle fibre can produce by electrical stimulation at different constant lengths. The classic FLR (figure 1, straight lines) [2] with its strikingly linear segments has been described not only up to the fibre level but also for the whole muscle [7,8]. Despite the fact that this relationship represents basic textbook knowledge for life science students, to date a convincing structural model explaining the shape of the entire FLR does not exist.

According to the sliding filament [4,5] and crossbridge [6] theories, actin and myosin filaments slide relative to each other in response to forces generated by temporary crossbridges formed by myosin heads—projecting from the myosin filaments—and actin filaments. This yields straightforward geometric explanations for the plateau region and for the region of decreasing isometric force based on filament lengths (figure 1, black lines) [2]. The slope change (figure 1, black circle) in the range of increasing isometric force (ascending limb) is typically related to myosin filaments hitting the Z-disc, a thin-meshed filament structure [9] defining the sarcomere boundary. It is, however, not clear which mechanism(s) are responsible for the decrease in force in the shallow and the steep slope regions of the ascending limb of the FLR [2,10–13].

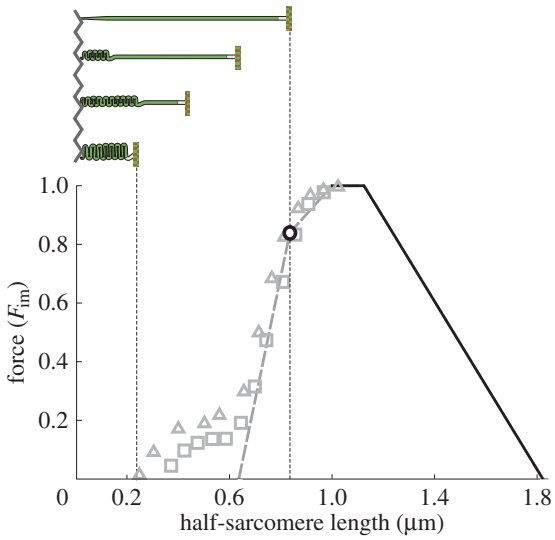

Figure 1. Isometric force over half-sarcomere length. Force is given as a fraction of maximum isometric force F_{im} (data by Gordon *et al.* [2] approximated as straight lines; data by Ramsey & Street [3] shown for two specimen as squares and triangles, respectively). The descending limb and the plateau (black lines) of this curve are directly predicted by the sliding filament [4,5] and crossbridge theories [6]. The slope change on the ascending limb (black circle) is related to the fibre length where myosin filaments reach the Z-disc. Explanation of the grey data is subject to scientific discussion (see text). The schematic half-sarcomere (top)—bounded by Z-disc (zigzag line) and M-line (vertical line)—illustrates required myosin filament (horizontal bar) compression or folding following the typical assumption that myosin filaments cannot penetrate the Z-disc. (Online version in colour).

More specifically, until now the ascending limb's steep slope is typically explained with myosin filament folding or compression (figure 1, top left scheme), and a possibly decreasing number of crossbridges [2,10,13]. An alternative recent explanation considers two-dimensional force production of crossbridges [14]. Ignoring that myosin filaments reach the Z-disc at the point of slope change on the ascending limb (figure 2, circle), their model predicts that the increasing filament lattice spacing leads to a considerable reduction in longitudinal force, explaining the slope of the steep part of the ascending limb. However, several studies suggest a minor impact of lattice spacing compatible with the whole working range of the fibre on longitudinal force [15,16].

In conflict with the ideas of an internal counteracting compression spring or lattice spacing being responsible for the steep slope of the ascending limb, Ramsey & Street [3] reported a pronounced FLR foot region for short fibre lengths (figure 1, symbols) produced in experiments with prolonged stimulus duration. Several phenomena were observed during and after fibre contractions within this range. Tension developed very slowly at short fibre lengths and was lower after re-elongation of the fibres. Moreover, unlike their regular behaviour, fibres did not restore their resting length after cessation of activation. These observations cannot be explained by myosin filament compression, lattice spacing or by a decreasing number of available crossbridges, and hence seemingly contradict the classic sliding filament and crossbridge theories of muscle contraction.

Here we develop a model consolidating structural and micromechanical data that can explain the entire FLR and resolve the apparent conflicts between experimental evidence and classic theories of contraction. The few required model parameters are taken from the literature or set by structural arguments. The model suggests mechanical causes for the tetragonal arrangement [9,17] of actin filaments at the Z-disc (in contrast with their hexagonal arrangement in the typical actin–myosin filament overlap), for the so far unknown function of the second myosin head [18], and for the ability of myosin heads to form crossbridges with actin filaments of opposite polarity [19,20].

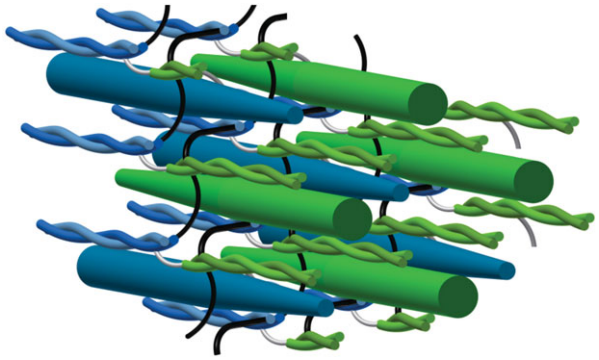

Figure 2. Myofilament arrangement after myosin filament sliding through the Z-disc. α-actinin molecules (black and grey) cross-link the tetragonal actin filament (helices) grids of opposite half-sarcomeres (green and blue, respectively) to form the Z-disc structure. Actin grids of opposite polarity are assumed to align as a consequence of myosin filament (thick rods) sliding through the Z-disc. Myosin filaments fill the previously empty spots within the chequered actin filament grid of the adjacent half-sarcomere. For further details on the sliding process, the Z-disc structure and the alignment of the actin grids, see text (see also figure 3; electronic supplementary material, figure S1 and text S1).

2. Myosin filament sliding through the Z-disc

The core of the model developed here is the idea that myosin filaments slide through the meshed Z-disc (figure 2 [21]) instead of being compressed or folded at short sarcomere lengths as typically assumed. This leads to several new types of actin–myosin filament overlap (figure 3*b–e*) affecting force production. In the following, we first introduce structural and geometrical arguments supporting the suggested mechanism and subsequently explain our model and its predictions (see Appendix A for mathematical details of the model).

The sliding of myosin filaments through the Z-disc requires a highly organized and sensibly adjusted geometry. First, the actin filament arrangement near the meshed Z-disc should be able to accommodate twice the number of myosin filaments within one half-sarcomere. The cross section of the typical actin–myosin overlap region reveals a hexagonal arrangement of actin filaments with a myosin filament centred in each actin hexagon (figure 3*a*, cross section **) [10,22]. Rearranging the actin filaments to a new regular lattice to accommodate twice the number of myosin filaments would require a tetragonal arrangement of actin filaments. Indeed, actin filament arrangement is tetragonal (square-cut) on either side of the meshed Z-disc (figure 3*a*, cross section *) [9,17].

Moreover, myosin filaments should be guided to form a regular pattern embedded in the tetragonal actin grid before reaching the Z-disc to enable orderly sliding through the Z-disc. Titin may be involved in fulfilling this task. Titin anchors myosin filaments to the Z-disc, and two titin

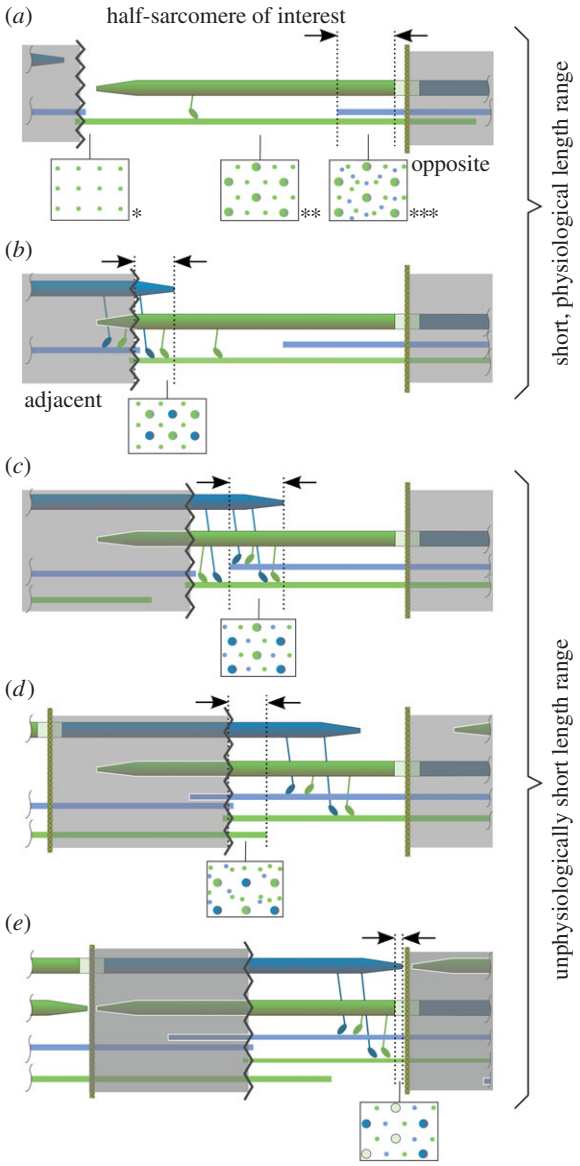

Figure 3. Schematic of proposed myosin (thick) and actin (thin) filament sliding. (*a*) Known [9,22,23] (cross sections *, **, ***) and (*b–e*) hypothesized filament arrangements and cross sections evolving during half-sarcomere shortening. (*a*) Starting from the plateau of the FLR, actin filaments from the opposite half-sarcomere passing the M-line enter the regular actin–myosin overlap, leading to actin–actin–myosin overlap. (*b*) Then myosin filaments from the adjacent half-sarcomere slide through the Z-disc, and a myosin–myosin–actin overlap zone evolves. (*c*) At even shorter length, the myosin–myosin–actin overlap zone meets the forthcoming actin–actin–myosin overlap zone, leading to actin–actin–myosin–myosin overlap. (*d*) Subsequently, actin filaments from the adjacent sarcomere enter the half-sarcomere of interest, leading to actin–actin–actin–myosin–myosin overlap. (*e*) Finally, the tips of myosin filaments from the adjacent half-sarcomere enter the myosin bare zone of the sarcomere of interest and eventually meet the M-line, where contraction is assumed to stop. Myosin heads projecting from the myosin filaments adjust to the polarity of the actin filament [19,20]. Same-colour myosin and actin filament represent relative filament orientation in regular overlap. During a shortening contraction, myosin heads interacting with actin of the same colour act concentrically, while myosin heads interacting with actin of a different colour act eccentrically.

molecules connect to each actin filament within the Z-disc [24]. Because the ratio of actin to myosin filaments is 2 : 1 in regular overlap (figure 3*a*, cross section **), the ratio of titin proteins to myosin filaments is 4 : 1. A simple possible symmetry (accounting for the two titin molecules per actin filament) in the myofilament arrangement is when each myosin filament connects via four titin proteins to four actin filaments forming the vertices of a square, resulting in a centred chequered arrangement of myosin filaments within the tetragonal actin grid. This arrangement would facilitate highly organized myosin filament sliding through the Z-disc, with the myosin filaments possibly entering the empty squares within the actin filament grid of the adjacent half-sarcomere (figure 2).

Although a comparably dense structure [24], the Z-disc adapts in diameter when the muscle changes in length (e.g. [25]) and is essentially porous [17]. Actin filament ends of opposite polarity are cross-linked by α-actinin (35 nm long molecules), forming a flexible basket weave pattern in activated muscle [17,26]. This structure offers a sufficient number of channels required for myosin filaments passing the Z-disc (figure 2; electronic supplementary material, figure S1). However, preceding the proposed sliding, actin filament grids of opposite polarity from neighbouring sarcomeres are not aligned at the Z-disc but are shifted by half a grid cell (approx. 20 nm; electronic supplementary material, figure S1). Subtleties within the Z-disc structure [17] break the symmetry of the basket weave pattern, which may help to align the neighbouring actin filament grids during the sliding process (see electronic supplementary material, figure S1 and text S1). This may result in a myofilament configuration after sliding through the Z-disc similar to that shown in figure 2.

Tapered myosin filament ends [27] facilitate entering the meshed Z-disc and help to take advantage of subtle asymmetries mentioned above. Moreover, with shortening, the width of a sarcomere increases due to the preservation of volume in muscle [28]. Similarly, the Z-disc may expand laterally by unfolding its spatial zigzag structure facilitated by lower forces pulling on the actin filaments (figure 1), making room for the increasingly thicker myosin filaments sliding through the Z-disc. Despite the increased number of filaments in the developing overlaps (figure 3*b–e*), the lateral distance between actin and myosin filaments would be at least 90% of their distance at optimal length in the regular overlap arrangement (see electronic supplementary material, text S2).

3. The model and its predictions

In our half-sarcomere model, active isometric force is proportional to the effective actin–myosin overlap length where force can be generated by crossbridges. This effective length refers to the standard hexagonal arrangement of actin filaments surrounding each myosin filament (figure 3*a*, cross section **). Different overlaps (indicated by arrows in figure 3) contribute with different strength to force production. In the actin–actin–myosin overlap (figure 3*a*; the number of repetitions of the filaments' names in the description of overlaps refers to the number of filaments in relation to regular overlap, i.e. actin–actin–myosin overlap contains twice the number of actin filaments and the identical number of myosin filaments like the regular overlap region), actin is abundant and seems to impede force production [13]. This result is extrapolated to the newly developing overlap in figure 3*d*, where actin filaments are also abundant. Because actin polarity determines the direction of action of

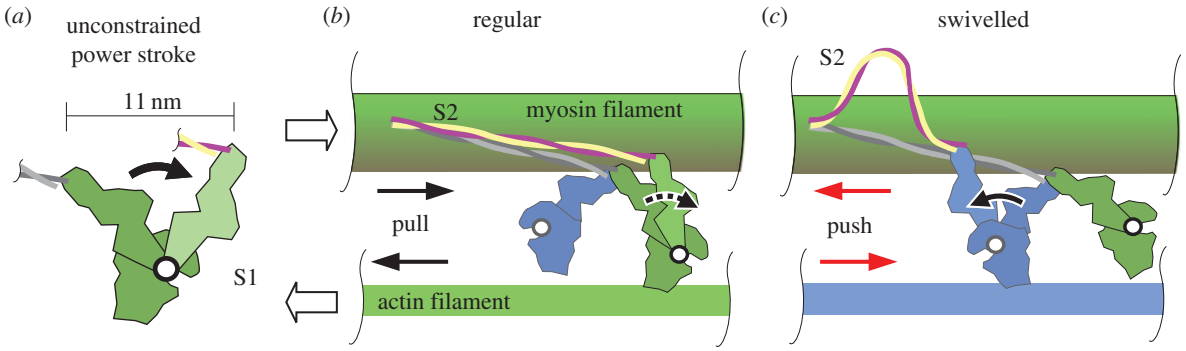

Figure 4. Illustration of proposed crossbridge action. (*a*) The full, unconstrained power stroke of the myosin S1 region covers 11 nm [28]. (*b*) The two myosin heads of one myosin molecule are shown in green and blue, respectively. Stiff myofilaments (actin and myosin) and no relative myofilament movement are assumed in an isometric (constant length) contraction. During the regular crossbridge power stroke of the green myosin head, its S1 region performs a sub-step of the unconstrained power stroke and deforms itself because the S2 region is stiff when pulled [29,30]. The crossbridge force tends to shorten the sarcomere (relative filament movement for fibre shortening indicated by unfilled arrows). (*c*) The swivelled crossbridge (blue) is formed because of flipped polarity of actin filaments (blue) compared with that in regular overlap. In contrast with the regular crossbridge, the swivelled crossbridge pushes the myofilaments, tending to elongate the sarcomere (red arrows). This leads to compression and buckling of the S2 region as a consequence of the power stroke because of low S2 compressive strength [29].

the crossbridges [19,20], half of the crossbridges in the remaining overlaps (figure 3*b*,*c*,*e*) would tend to shorten the sarcomere while the other half, the swivelled crossbridges [20], would tend to lengthen the sarcomere (figure 4). Assuming that the swivelled crossbridges produce the same force as their regular counterparts, the resulting isometric force in these overlaps equals zero, and the model generates an FLR (figure 5, *prediction I*) remarkably similar to the classic FLR (grey dotted lines).

However, the crossbridge is much softer in pushing than in pulling [29] (figure 4). From experimental data [29,30,33], we estimate (see electronic supplementary material, text S3) that the pushing force of a swivelled crossbridge in an isometric contraction is approximately half the pulling force of a regular crossbridge. Considering further the number of myosin filaments interacting with each actin filament for each overlap, the model predicts an FLR (figure 5, *prediction II*) that corresponds well with the classic experimental FLR, and—in the foot region below the length of classic zero force—with the data of Ramsey & Street [3] (figure 5, symbols).

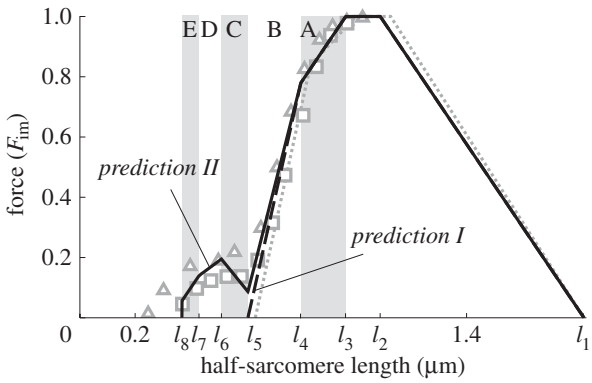

Figure 5. Comparison of model-predicted force–length relationship (black lines) and data (grey). *Prediction I* assumes that regular and swivelled crossbridges produce equal forces. *Prediction II* assumes that swivelled crossbridges produce half the force of regular crossbridges (see figure 4; electronic supplementary material, text S3). Overlap regions with abundant actin are assumed to produce no force [13]. Parameters used for the geometric model are myosin filament length 1.6 μm [31], bare region length of the myosin filaments 0.125 μm (lower range of reported values) [32], Z-disc width 0 μm, and actin filament length 1.025 μm (calculated from fully extended sarcomere length $l_1 = 3.65$ μm, [2]). Ranges A–E correspond to figure 3*a*–*e*, half-sarcomere lengths l_1–l_8 correspond to equation (A 2).

4. Discussion

Our simple muscle model effortlessly explains the stunning linearity of the segments of the classic force–length relationship (FLR) of striated muscle (figure 5, *prediction I*). It is based on the idea that myosin filaments slide through the Z-disc [21] (figure 2) instead of being compressed or folded at the Z-disc as commonly assumed. By this elegant mechanism, the muscle can maintain its highly organized structure at short lengths (figure 5, range B) occurring regularly during daily activities [34]. Considering decreased swivelled relative to regular crossbridge forces, the model predicts as yet puzzling force production at lengths shorter than the length of classic zero force [3] (figure 5, *prediction II*, ranges C–E). It seems noteworthy that the good agreement of the model predictions and data were achieved without fitting of parameters; instead, parameters were obtained from the literature or set by structural arguments (cf. Appendix A; electronic supplementary material, text S3). Decreased relative swivelled crossbridge force decreases the FLR's ascending limb's slope in our model (figure 5). This effect may be compensated by increasing filament lattice spacing tending to increase the slope in this range [14]. Although direct micrographic evidence is scarce [21], a range of micromechanical, biophysical and structural evidence supports the theory.

(a) Flexural stiffness of myofilaments

The suggested mechanism relies on sufficient flexural stiffness of the myofilaments. The myosin filaments should not buckle when passing the Z-disc (figure 2) or when transmitting compressive force due to eccentric crossbridges (figure 3*b*–*e*). Conservative estimates of critical buckling force of myosin filaments based on experimental data (see electronic supplementary material, text S4) yield values of 0.90–1.33 nN, about three to four times the maximum isometric force in a myosin filament [35]. Moreover, muscle force decreases with contraction speed [36]. Hence myosin filament buckling

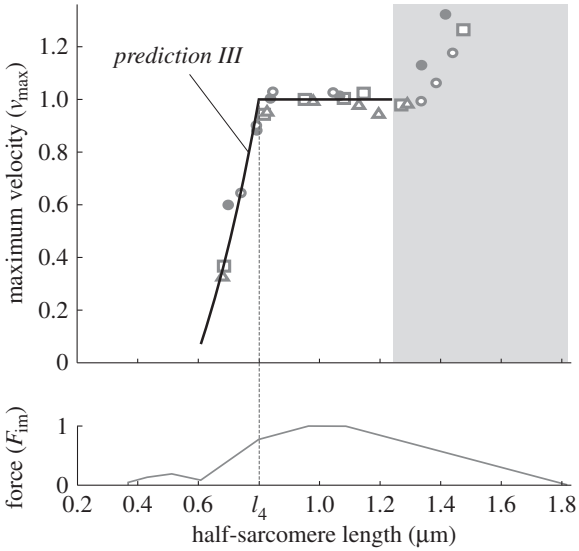

Figure 6. Comparison of model-predicted maximum half-sarcomere contraction velocity (black line) and data (symbols [38]). The model and the data show a similar decrease of maximum contraction velocity for half-sarcomere lengths smaller than l_4. For orientation, the force–length relationship is depicted below. The maximum half-sarcomere contraction velocity is normalized to v_{max}, its value in the plateau range of the force–length relationship. The increase in maximum contraction velocity in the grey shaded area stems from passive forces [38] not considered in our model.

seems rather unlikely; vice versa, myosin filament stiffness seems to be a crucial filament property, suggesting that myosin filaments cannot be folded or even compressed at the meshed Z-disc.

In comparison, actin filaments are much more flexible (approx. 70-fold) than myosin filaments [37]. Still, actin filaments are sufficiently stiff to pass the sarcomere's M-line, and—after unphysiological detachment from the Z-disc—they can be pushed like rods to the opposing Z-disc by crossbridges acting at their ends [13]. Their flexural stiffness may become relevant within range C (figure 5) when swivelled crossbridges would compress actin filaments (figure 3*c*, green myosin head on blue actin filament).

(b) Prediction of maximum contraction velocity

Otherwise constant maximum contraction velocity of sarcomeres in regions of zero passive force is known to decrease linearly for half-sarcomere lengths shorter than length l_4 [38] (figure 6, symbols). Swivelled crossbridges (figure 4*c*) formed when myosin filaments slide through the Z-disc into the adjacent half-sarcomere during half-sarcomere shortening slow down the contraction. Accounting for the force–velocity relation of muscle [36,39], our model even quantitatively predicts the reported behaviour of maximum contraction velocity in frog muscle (figure 6, *prediction III*; see electronic supplementary material, text S5), which supports the concept of myosin filament sliding through the Z-disc.

(c) 'Strange' behaviour of muscle fibres

In early kinetic experiments on muscle fibres, Ramsey & Street [3] reported puzzling behaviour of muscle fibres at very short fibre lengths (figure 5, ranges C–E) and postulated that fibres enter a so-called 'delta state'. The described slow development of force when entering range C coincides with the development of the new myosin–myosin–actin–actin overlap (figure 3*c*). Considering the flexural stiffness of the myofilaments (see above), it is unclear how this presumed overlap should seamlessly develop from the two different adjacent overlaps with triangular myosin filament lattice on one side (actin–actin–myosin overlap; figure 3*a*, cross section ***) and tetragonal myosin filament lattice on the other side (myosin–myosin–actin overlap; figure 3*b*). Myofilaments might interlock due to increased friction as a result of disordered filament sliding. This could be a contributing factor to the explanation of why fibres did not restore their resting length after cessation of activation [3]. If such a fibre is re-elongated, locked half-sarcomeres may, one by one, pop to a long length where passive half-sarcomere structures would take up the stretching force. In a subsequent end-held isometric contraction, the fibre might exert less force than expected (as observed [3]) because of overstretched half-sarcomeres and compensating motions of half-sarcomeres accompanying force equilibration. Accordingly, if the whole fibres would be passively overstretched after entering the 'delta state', all stuck half-sarcomeres would elongate and they would restore their resting length, as seen in experiments [3].

Myosin-binding protein C, a thick filament protein that presumably bridges actin and myosin filaments [40], may also contribute to the described phenomenon of locked half-sarcomeres. Intriguingly, in frog myosin filaments this large protein occurs in 43 nm intervals from approximately 250 to 500 nm (measured from the M-line) along the myosin filament [40]. Hence, according to our model, the first layer of myosin-binding protein C would reach the Z-disc in range C (figure 5). It is feasible that over time myosin-binding protein C gets pulled through the Z-disc in activated muscle and then prevents passive re-elongation of the muscle to resting length when activation ceases (e.g. due to friction).

Although performed in part at unphysiological lengths, the measurements by Ramsey & Street [3] potentially contain important clues to the functioning of the contractile machinery of the muscle fibre in the physiological range. Because some doubt remains with respect to reproducibility and hence relevance of the findings by Ramsey & Street [3] obtained with frog muscle fibres for the general functioning of vertebrate muscle fibres, we repeated parts of their experiments with fibres of the rat *M. extensor digitorum longus* (figure 7). We likewise found considerable force development of the fibres for long duration of activation at lengths shorter (0.53 µm half-sarcomere length) than classical zero force (0.63 µm half-sarcomere length; figure 1 [2]). Also, fibres did not restore their resting lengths and produced less force when re-elongated, but full force after being passively overextended. Moreover, Schoenberg & Podolsky [42] also measured forces at half-sarcomere lengths of 0.5–0.6 µm. There is increasing evidence that these results are not artefacts but properties of vertebrate fibres; myosin filament sliding through the Z-disc is an appealing possibility that reconciles them with current theories of contraction.

(d) Swivelled crossbridges and evolution

More than half a billion years ago, striated muscles presumably appeared in our prebilaterian ancestors [43]. Prior to the existence of exo- and endoskeletal structures, muscles probably adhered to gelatinous material such as is present,

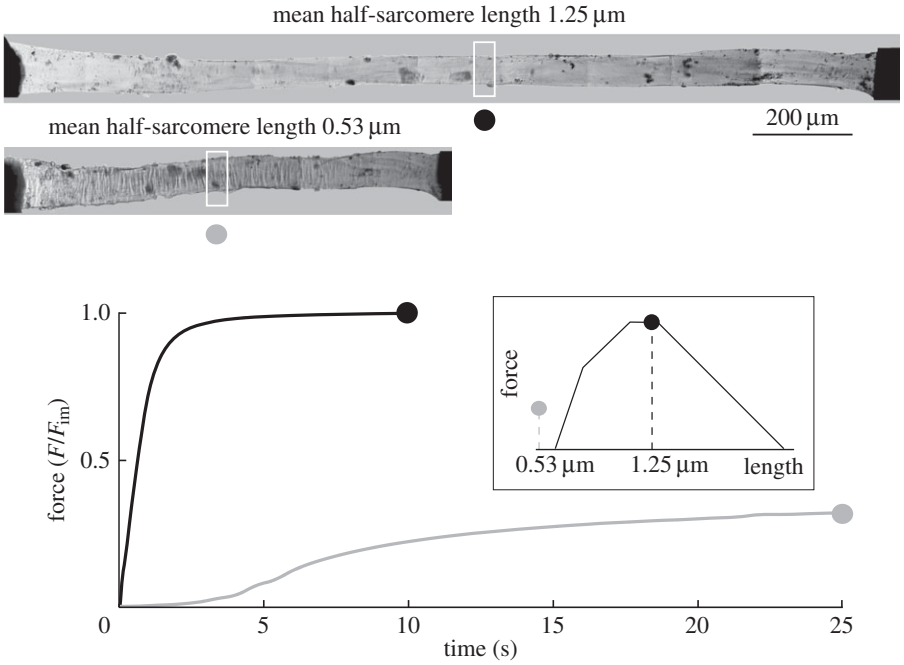

Figure 7. Isometric measurements with a segment of a single muscle fibre of rat *M. extensor digitorum longus* show considerable force at lengths below classic zero force for extended activation. Force–time traces generated by the muscle fibre at optimum (1.25 µm, black line) and short (0.53 µm, grey line) half-sarcomere lengths. Preparation and fixation of fibres followed the protocol of Goldman & Simmons [41]. The permeabilized fibre was maximally (pCa 4.5) activated for 10 s and 25 s at 1.25 µm and 0.53 µm, respectively, at 12°C. Force was measured using a fibre test apparatus (Aurora Scientific, 1400A). Mean sarcomere length was measured microscopically (Nikon Ti-S, 500×) within the white boxed part of the fibre (top graphs) with a high-speed video system for sarcomere length measurement (Aurora Scientific, 901B). Calcium activation started at time $t = 0$. At very short, unphysiological half-sarcomere length (0.53 µm), the muscle fibre segment is initially slack (it sags). After pulling in the slack, the fibre segment becomes taut and force develops slowly. Force reached about 30% of maximum isometric force (F_{im}) at the end of activation. In the inset, the measured steady-state lengths and forces can be compared with the rat's theoretical force–length relationship (obtained with the same parameters as in figure 6 but with longer rat actin length of 1.13 µm [32]).

for instance, in sponge and jellyfish [43]. Therefore, the muscle had to be equipped with a safety mechanism preventing extreme shortening and muscle malfunction, as described above. The swivelled crossbridges damping muscle contraction at short lengths represent such a safety mechanism. On a related note, this phenomenon may explain the so far unknown function of the second parallel myosin head attached to each myosin molecule [18], which may generate the swivelled crossbridges. However, this function comes at a metabolic cost. In species with skeletons, evolution may have adjusted the region of operation of the muscle by tuning origin and insertion such that it avoids damping its own contraction. For example, floating species such as fish can function more in the plateau region of the FLR [34] than non-floating species. In floating species, postural stability is provided by the aquatic environment. By contrast, species acting with their musculoskeletal system against gravity seem to make use of this 'old' muscle function by selected muscles operating in the range of the steep part of the ascending limb of the FLR [34], potentially to increase stability and to facilitate docile behaviour towards perturbations.

5. Conclusion

The assumption of myosin filament folding or even compression (which would need to exceed 60% for extreme cases of muscle shortening; figure 1) commonly used in textbooks cannot explain (i) how force can be produced at lengths shorter than the length of classic zero force; (ii) why the muscle does not restore its resting length after contractions with extended activation duration; and (iii) how the stiff myosin filaments can be folded or compressed at a meshed Z-disc. Accepting the idea that myosin filaments slide through the Z-disc and incorporating this mechanism into a comparably simple model with comprehensible, few parameters reconcile these data with classic theories of contraction.

In addition, the model enables new perspectives on the relation between striated fibre structure and its mechanical function. The transformation from hexagonal to tetragonal actin filament lattice near the Z-disc enables the development of an orderly myofilament structure at short fibre lengths. The Z-disc becomes an integral part of the contractile mechanism. For example, eccentric exercise [44] or muscle diseases like Duchenne muscular dystrophy or Sjögren's syndrome are accompanied by a loss of structural integrity of the Z-disc. This may result in disordered myosin sliding through the Z-disc, contributing to the observed muscle weakness. A more comprehensible understanding of muscle structure and function seems within reach.

Authors' contributions. C.R. developed the ideas, performed the research, analysed the data and drafted the manuscript. T.S. contributed to the ideas, supervised the experiments and helped draft the manuscript. A.T. performed the experiments. R.B. contributed micromechanical considerations and helped draft the manuscript. All authors gave final approval for publication.

Competing interests. We have no competing interests.

Funding. We received no funding for this study.

Acknowledgement. The authors thank Anvar Jakupov for technical help with figure 2.

Appendix A. The model

Active isometric half-sarcomere force F depends on half-sarcomere length l_{hs} and is proportional to an effective actin–myosin overlap region l_{eff}, where force can be generated by crossbridges. Normalizing this length to the maximum effective actin–myosin filament overlap length (l_{effmax}, the zone of myosin heads in a half-myosin), we obtain the isometric force as percentage of maximum isometric half-sarcomere force F_{im} at optimal fibre length:

$$\frac{F(l_{hs})}{F_{im}} = \frac{l_{eff}(l_{hs})}{l_{eff\,max}}. \tag{A 1}$$

The Z-disc is assumed to have zero depth. Then, starting from long lengths, half-sarcomere lengths l_1 (no actin–myosin overlap), l_2 (start of plateau), l_3 (start of shallow slope), l_4 (start of steep slope), l_5 (actin–actin–myosin overlap meets myosin–myosin–actin overlap), l_6 (actin filaments of adjacent half-sarcomere meet Z-disc), l_7 (myosin filaments of adjacent half-sarcomeres meet bare zone) and l_8 (myosin filaments of adjacent half-sarcomeres meet M-line) are given by

$$\left.\begin{aligned} l_1 &= l_a + \frac{l_m}{2},\\ l_2 &= l_a + \frac{l_{bare}}{2},\\ l_3 &= l_a - \frac{l_{bare}}{2},\\ l_4 &= \frac{l_m}{2},\\ l_5 &= \frac{2l_a + l_m}{6},\\ l_6 &= \frac{l_a}{2},\\ l_7 &= \frac{l_m + l_{bare}}{4}\\ \text{and}\quad l_8 &= \frac{l_m - l_{bare}}{4}, \end{aligned}\right\} \tag{A 2}$$

with actin filament length l_a, myosin filament length l_m and the bare zone length without myosin heads at the centre of the myosin filament l_{bare}. Each different overlap region (figure 3, between arrows) is scaled by an individual factor c to a corresponding length of regular overlap (i.e. three myosin filaments interact with each actin filament tending to shorten the sarcomere); the sum of the scaled lengths yields the effective overlap length

$$l_{eff}(l_{hs}) = \begin{cases} (l_1 - l_{hs}), & l_2 \le l_{hs} \le l_1\\ (l_1 - l_2), & l_3 \le l_{hs} < l_2\\ \left(\frac{l_m}{2}2 + l_{hs} - l_a\right) + c_{aam}(l_3 - l_{hs}), & l_4 \le l_{hs} < l_3\\ \left(3l_{hs} - l_a - \frac{l_m}{2}\right) + c_{aam}(l_3 - l_{hs}) + c_{mma}(l_m/2 - l_{hs}), & l_5 \le l_{hs} < l_4\\ c_{aam}\left(2l_{hs} - \frac{l_m}{2} - \frac{l_{bare}}{2}\right) + c_{mma}(2l_{hs} - l_a) + c_{aamm}\left(l_a + \frac{l_m}{2} - 3l_{hs}\right), & l_6 \le l_{hs} < l_5\\ c_{aam}\left(2l_{hs} - \frac{l_m}{2} - \frac{l_{bare}}{2}\right) + c_{aamm}\left(\frac{l_m}{2} + l_{hs} - l_a\right) + c_{aaamm}(l_a - 2l_{hs}), & l_7 \le l_{hs} < l_6\\ c_{aamm}\left(3l_{hs} - l_a - \frac{l_{bare}}{2}\right) + c_{aaamm}(l_a - 2l_{hs}) + c_{aamm*}(2l_7 - 2l_{hs}) & l_8 \le l_{hs} < l_7. \end{cases} \tag{A 3}$$

The index of c denotes the corresponding overlap region. For instance, c_{aamm} scales the actin–actin–myosin–myosin overlap (figure 3*c*). The asterisk in the bottom row of equation (A 3) indicates its quantitative change within the bare zone of myosin of the half-sarcomere of interest where only half of myosin heads are available (figure 3*e*).

Calculating *prediction I* (figure 5), all c factors equal zero. For calculating *prediction II* (figure 5) and *prediction III* (figure 6), c factors consider the available number of actin filaments, the number of myosin filaments interacting with each actin filament and the orientation of the crossbridges. c_{aam} and c_{aaamm} were set to zero because experiments indicate that force is zero when actin filaments are abundant [13]. From the cross sections in figure 3*b*,*c*,*e*, we count how many myosin filaments produce regular (M_r) and swivelled crossbridges (M_s) with each actin, respectively. Sectors M_s tending to lengthen the sarcomere produce half the force ($f = 0.5$; see electronic supplementary material, text S3) of filament sectors M_r, tending to shorten the sarcomere. Thus, we subtract the number of M_s per actin filament scaled by f from M_r per filament and divide this difference by three (the number of myosin filaments per actin tending to shorten the sarcomere in regular overlap). Finally, this number is multiplied by A (the number of available actin filaments divided by the number of actin filaments in regular overlap) to yield individual c:

$$c = A \cdot \frac{M_r - f \cdot M_s}{3}. \tag{A 4}$$

According to the mechanism of myosin sliding through the Z-disc (figure 2), we expect a regular tetragonal pattern of actin filaments and myosin filaments within the myosin–myosin–actin overlap (figures 2 and 3*b*, cross section). Within this overlap region, two myosin filaments from the current half-sarcomere and two myosin filaments from the adjacent half-sarcomere (forming swivelled crossbridges) act on each actin filament. Hence, $c_{mma} = 1(2 - 0.5 \cdot 2)/3 = 0.33$. In the actin–actin–myosin–myosin overlap the actin–myosin filament ratio is 2 : 1. Though formation of a regular structure may be inhibited (see Discussion), for the sake of

simplicity we assume the development of a hexagonal actin filament arrangement similar to the regular overlap zone. Here, on average, 1.5 myosin filaments per actin filament tend to shorten the sarcomere, and 1.5 myosin filaments per actin filament tend to extend the sarcomere. Because there are twice as many actin filaments compared with regular overlap, this results in $c_{\mathrm{aamm}} = 2\ (1.5 - 0.5 \cdot 1.5)/3 = 0.5$. Accordingly, the actin–actin–myosin–myosin overlap within the bare zone of one set of myosin filaments must be scaled by $c_{\mathrm{aamm}^*} = 0.25$.

References

1. Blix M. 1891 Die Länge und die Spannung des Muskels. *Skand. Arch. Physiol.* **3**, 295–118. (doi:10.1111/j.1748-1716.1892.tb00660.x)
2. Gordon AM, Huxley AF, Julian FJ. 1966 The variation in isometric tension with sarcomere length in vertebrate muscle fibres. *J. Physiol.* **184**, 170–192. (doi:10.1113/jphysiol.1966.sp007909)
3. Ramsey RW, Street SF. 1940 The isometric length-tension diagram of isolated skeletal muscle fibers of the frog. *J. Cell. Compar. Physiol.* **15**, 11–34. (doi:10.1002/jcp.1030150103)
4. Huxley H, Hanson J. 1954 Changes in the cross-striations of muscle during contraction and stretch and their structural interpretation. *Nature* **173**, 973–976. (doi:10.1038/173973a0)
5. Huxley AF, Niedergerke R. 1954 Structural changes in muscle during contraction: interference microscopy of living muscle fibres. *Nature* **173**, 971–973. (doi:10.1038/173971a0)
6. Huxley AF. 1957 Muscle structure and theories of contraction. *Prog. Biophys. Biophys. Chem.* **7**, 255–318.
7. Rode C, Siebert T, Herzog W, Blickhan R. 2009 The effects of parallel and series elastic components on the active cat soleus force–length relationship. *J. Mech. Med. Biol.* **9**, 105–122. (doi:10.1142/S0219519409002870)
8. Winters TM, Takahashi M, Lieber RL, Ward SR. 2011 Whole muscle length-tension relationships are accurately modeled as scaled sarcomeres in rabbit hindlimb muscles. *J. Biomech.* **44**, 109–115. (doi:10.1016/j.jbiomech.2010.08.033)
9. Knappeis GG, Carlsen F. 1962 The ultrastructure of the Z disc in skeletal muscle. *J. Cell Biol.* **13**, 323–335. (doi:10.1083/jcb.13.2.323)
10. MacIntosh BR, Gardiner PF, McComas AJ. 2006 *Skeletal muscle: form and function*, 2nd edn. Champaign, IL: Human Kinetics.
11. Allen JD, Moss RL. 1987 Factors influencing the ascending limb of the sarcomere length-tension relationship in rabbit skinned muscle fibres. *J. Physiol.* **390**, 119–136. (doi:10.1113/jphysiol.1987.sp016689)
12. Scott SH, Brown IE, Loeb GE. 1996 Mechanics of feline soleus. I. Effect of fascicle length and velocity on force output. *J. Muscle Res. Cell Motil.* **17**, 207–219. (doi:10.1007/BF00124243)
13. Trombitas K, Tigyi-Sebes A. 1984 Cross-bridge interaction with oppositely polarized actin filaments in double-overlap zones of insect flight muscle. *Nature* **309**, 168–170. (doi:10.1038/309168a0)
14. Williams CD, Salcedo MK, Irving TC, Regnier M, Daniel TL. 2013 The length–tension curve in muscle depends on lattice spacing. *Proc. R. Soc. B* **280**, 20130697. (doi:10.1098/Rspb.2013.0697)
15. Millman BM. 1998 The filament lattice of striated muscle. *Physiol. Rev.* **78**, 359–391.
16. Gulati J, Babu A. 1985 Critical dependence of calcium-activated force on width in highly compressed skinned fibers of the frog. *Biophys. J.* **48**, 781–787. (doi:10.1016/S0006-3495(85)83836-4)
17. Luther PK. 2000 Three-dimensional structure of a vertebrate muscle Z-band: implications for titin and alpha-actinin binding. *J. Struct. Biol.* **129**, 1–16. (doi:10.1006/jsbi.1999.4207)
18. Huxley AF. 2000 Cross-bridge action: present views, prospects, and unknowns. *J. Biomech.* **33**, 1189–1195. (doi:10.1016/S0021-9290(00)00060-9)
19. Toyoshima YY, Toyoshima C, Spudich JA. 1989 Bidirectional movement of actin filaments along tracks of myosin heads. *Nature* **341**, 154–156. (doi:10.1038/341154a0)
20. Reedy MC, Beall C, Fyrberg E. 1989 Formation of reverse rigor chevrons by myosin heads. *Nature* **339**, 481–483. (doi:10.1038/339481a0)
21. Hagopian M. 1970 Contraction bands at short sarcomere length in chick muscle. *J. Cell Biol.* **47**, 790–796. (doi:10.1083/jcb.47.3.790)
22. Huxley HE. 1957 The double array of filaments in cross-striated muscle. *J. Biophys. Biochem. Cytol.* **3**, 631–648. (doi:10.1083/jcb.3.5.631)
23. Trombitas K, Tigyi-Sebes A. 1985 How actin filament polarity affects crossbridge force in doubly-overlapped insect muscle. *J. Muscle Res. Cell Motil.* **6**, 447–459. (doi:10.1007/BF00712582)
24. Zou P, Pinotsis N, Lange S, Song YH, Popov A, Mavridis I, Mayans OM, Gautel M, Wilmanns M. 2006 Palindromic assembly of the giant muscle protein titin in the sarcomeric Z-disk. *Nature* **439**, 229–233. (doi:10.1038/nature04343)
25. Huxley HE. 1953 X-ray analysis and the problem of muscle. *Proc. R. Soc. Lond. B* **141**, 59–62. (doi:10.1098/rspb.1953.0017)
26. Goldstein MA, Michael LH, Schroeter JP, Sass RL. 1988 Structural states in the Z band of skeletal muscle correlate with states of active and passive tension. *J. Gen. Physiol.* **92**, 113–119. (doi:10.1085/jgp.92.1.113)
27. Luther PK, Munro PM, Squire JM. 1981 Three-dimensional structure of the vertebrate muscle A-band. III. M-region structure and myosin filament symmetry. *J. Mol. Biol.* **151**, 703–730. (doi:10.1016/0022-2836(81)90430-7)
28. Swammerdam J. 1737 *Biblia naturae*. Leiden: Isaak Severinus, Boudewyn and Peter vander Aa.
29. Kaya M, Higuchi H. 2010 Nonlinear elasticity and an 8-nm working stroke of single myosin molecules in myofilaments. *Science* **329**, 686–689. (doi:10.1126/science.1191484)
30. Brunello E *et al.* 2014 The contributions of filaments and cross-bridges to sarcomere compliance in skeletal muscle. *J. Physiol. Lond.* **592**, 3881–3899. (doi:10.1113/jphysiol.2014.276196)
31. Craig R. 1977 Structure of a-segments from frog and rabbit skeletal muscle. *J. Mol. Biol.* **109**, 69–81. (doi:10.1016/S0022-2836(77)80046-6)
32. ter Keurs HE, Luff AR, Luff SE. 1984 Force–sarcomere-length relation and filament length in rat extensor digitorum muscle. *Adv. Exp. Med. Biol.* **170**, 511–525. (doi:10.1007/978-1-4684-4703-3_44)
33. Finer JT, Simmons RM, Spudich JA. 1994 Single myosin molecule mechanics: piconewton forces and nanometre steps. *Nature* **368**, 113–119. (doi:10.1038/368113a0)
34. Burkholder TJ, Lieber RL. 2001 Sarcomere length operating range of vertebrate muscles during movement. *J. Exp. Biol.* **204**, 1529–1536.
35. Rode C, Siebert T, Blickhan R. 2009 Titin-induced force enhancement and force depression: a 'sticky-spring' mechanism in muscle contractions? *J. Theor. Biol.* **259**, 350–360. (doi:10.1016/j.jtbi.2009.03.015)
36. Hill AV. 1938 The heat of shortening and the dynamic constants of muscle. *Proc. R. Soc. Lond. B* **126**, 136–195. (doi:10.1098/rspb.1938.0050)
37. Miller MS, Tanner BC, Nyland LR, Vigoreaux JO. 2010 Comparative biomechanics of thick filaments and thin filaments with functional consequences for muscle contraction. *J. Biomed. Biotechnol.* **2010**, 473423. (doi:10.1155/2010/473423)
38. Edman KA. 1979 The velocity of unloaded shortening and its relation to sarcomere length and isometric force in vertebrate muscle fibres. *J. Physiol.* **291**, 143–159. (doi:10.1113/jphysiol.1979.sp012804)
39. Till O, Siebert T, Rode C, Blickhan R. 2008 Characterization of isovelocity extension of activated muscle: a hill-type model for eccentric contractions and a method for parameter determination. *J. Theor. Biol.* **255**, 176–187. (doi:10.1016/j.jtbi.2008.08.009)
40. Luther PK, Winkler H, Taylor K, Zoghbi ME, Craig R, Padron R, Squire J.M, Liu J. 2011 Direct visualization of myosin-binding protein C bridging myosin and actin filaments in intact muscle. *Proc. Natl Acad. Sci.*

USA **108**, 11 423–11 428. (doi:10.1073/pnas.1103216108)

41. Goldman YE, Simmons RM. 1984 Control of sarcomere-length in skinned muscle-fibers of *Rana temporaria* during mechanical transients. *J. Physiol. Lond.* **350**, 497–518. (doi:10.1113/jphysiol.1984.sp015215)
42. Schoenberg M, Podolsky RJ. 1972 Length–force relation of calcium activated muscle fibers. *Science* **176**, 52–54. (doi:10.1126/science.176.4030.52)
43. Seipel K, Schmid V. 2005 Evolution of striated muscle: jellyfish and the origin of triploblasty. *Dev. Biol.* **282**, 14–26. (doi:10.1016/j.ydbio.2005.03.032)
44. Lieber RL, Friden J. 2002 Mechanisms of muscle injury gleaned from animal models. *Am. J. Phys. Med. Rehabil.* **81**(11 Suppl.), S70–S79. (doi:10.1097/00002060-200211001-00008)